



THE UNIVERSITY *of* EDINBURGH

Edinburgh Research Explorer

## Characterisation of Epoxy Powders for Processing Thick-Section Composite Structures

**Citation for published version:**

Maguire, J, Nayak, K & O Brádaigh, C 2018, 'Characterisation of Epoxy Powders for Processing Thick-Section Composite Structures', *Materials & Design*, vol. 139, pp. 112-121.  
<https://doi.org/10.1016/j.matdes.2017.10.068>

**Digital Object Identifier (DOI):**

[10.1016/j.matdes.2017.10.068](https://doi.org/10.1016/j.matdes.2017.10.068)

**Link:**

[Link to publication record in Edinburgh Research Explorer](#)

**Document Version:**

Peer reviewed version

**Published In:**

Materials & Design

**General rights**

Copyright for the publications made accessible via the Edinburgh Research Explorer is retained by the author(s) and / or other copyright owners and it is a condition of accessing these publications that users recognise and abide by the legal requirements associated with these rights.

**Take down policy**

The University of Edinburgh has made every reasonable effort to ensure that Edinburgh Research Explorer content complies with UK legislation. If you believe that the public display of this file breaches copyright please contact [openaccess@ed.ac.uk](mailto:openaccess@ed.ac.uk) providing details, and we will remove access to the work immediately and investigate your claim.



# Characterisation of epoxy powders for processing thick-section composite structures

James. M. Maguire <sup>a,\*</sup>, Kapileswar Nayak <sup>b</sup>, Conchúr M. Ó Brádaigh <sup>a</sup>

<sup>a</sup> School of Engineering, Institute for Materials and Processes, The University of Edinburgh, Edinburgh, EH9 3FB, UK

<sup>b</sup> SE Blades Technology B.V., Jan Tinbergenstraat 290, 7559 ST Hengelo (Overijssel), The Netherlands

\* Corresponding author. Email address: j.maguire@ed.ac.uk

## Abstract

Epoxy powders were investigated as a processing route for fast, low-cost manufacturing of thick-section fibre reinforced polymer parts. Thermogravimetric analysis (TGA), differential scanning calorimetry (DSC), and parallel-plate rheometry were used to characterise the material for realistic processing conditions. The epoxy powders contained heat-activated curing agents and exhibited good thermal stability at and above typical processing temperatures (160-180°C). The exothermic heat produced during curing was found to be small when compared to some conventional epoxies. Similarly, it was shown that epoxy powders can be melted between 45 and 120°C to achieve low viscosities for fibre tow impregnation, without inducing significant cure. Semi-empirical cure kinetics and chemorheological models were presented, which can be used to predict the epoxy's behaviour during part consolidation and curing. Modifications were made to an existing cure kinetics model to better represent the behaviour of the epoxy at lower temperatures. The relationship between glass transition temperature and the degree-of-cure was described using the DiBenedetto equation and was implemented in an existing chemorheological model. The chemorheological model was applied to a standard process cycle to assess the accuracy of the model and the effectiveness of the process cycle.

## Keywords

Polymer composites; Epoxy powder; Characterisation; Composite processing; Thick-section

## 1. Introduction

The composite materials industry continues to grow as demand increases for more lightweight, high strength products. In recent years, the composites manufacturing industry has looked towards out-of-autoclave (OOA) materials and processes as a more cost-effective way of producing high quality composite components. Examples include: high-pressure resin transfer moulding (HP-RTM), which has gained attention for its use by BMW in the iSeries production [1]; vacuum infusion processing (VIP), a commonly used technique in manufacturing wind turbine blades [2]; and vacuum-bag-only (VBO) prepregs, which have evolved from conventional autoclave prepregs and have been the topic of much research in the aerospace industry [3]. In the latter case, it has been shown that the latest generation of VBO prepregs can be used to manufacture autoclave-quality products without the need for expensive infrastructure and tooling. VBO prepregs typically consist of a fibre reinforcement that is *partially* impregnated with a thermoset resin matrix, whereas conventional autoclave prepregs are fully impregnated with resin. This leaves dry-fibre pathways in the VBO prepregs which allow air and vaporised moisture to be evacuated under vacuum conditions, thus reducing the likelihood of void formation [3]. Full consolidation of a part is achieved by applying sufficient heat to reduce the resin viscosity so that it can flow into the dry fibre tows (< 100 Pa.s [4]), as illustrated in Fig. 1. The plies of prepreg are consolidated by atmospheric pressure acting through the flexible vacuum bag. Heating the material can be achieved in numerous ways including large ovens and integrally heated tooling [5]. Commonly, carbon fibres are the reinforcement used in these VBO prepregs; however, the

technology can be extended to include other fibre types, such as glass and basalt, as a potential means of cost savings or to change the mechanical properties.

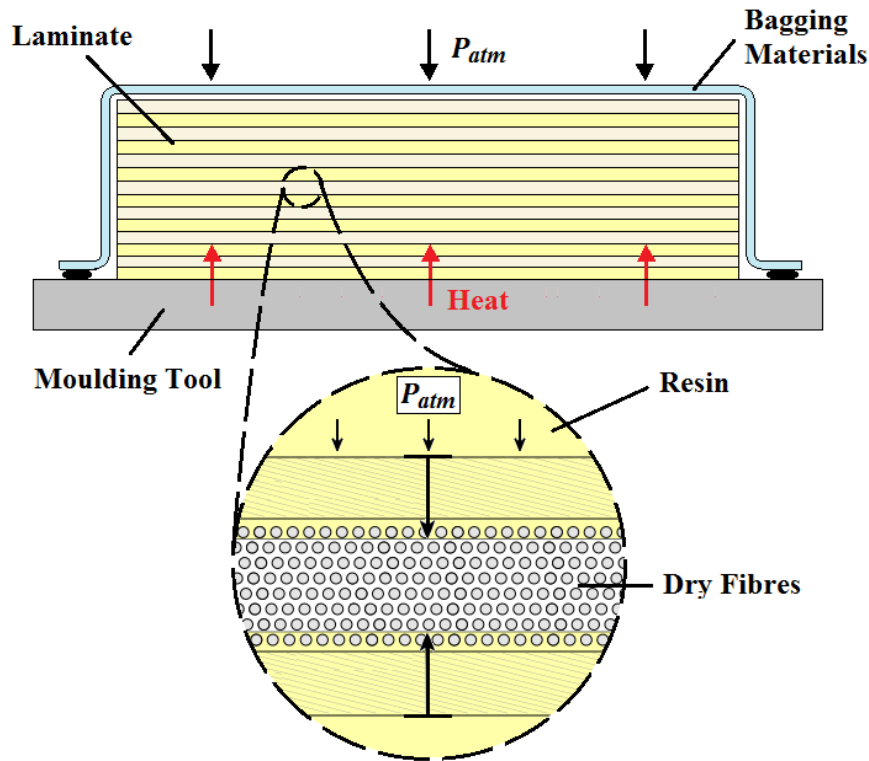


**Fig. 1.** Illustration of VBO prepreg processing; atmospheric pressure and heat are applied to the laminate. The enlarged image shows that the resin is forced to flow into the dry fibre layer and then cures to form the final part.

While much of the development for VBO prepregs has been focused on the aerospace industry, a number of companies have developed these type of prepregs and resins for use in marine and wind energy. Juska et al [6] highlighted that VBO prepregs are well suited to low volume production of large parts, as considerably less skill and labour are required when compared to vacuum infusion technologies. VBO prepregs for thick-section parts may be of particular importance to emerging industries such as the marine renewable energy (MRE) industry where the cost of wave energy converters (WECs) and blades for tidal energy converters (TECs) are a major barrier to the technology; materials and manufacturing has been targeted as an area for cost reduction [7].

As outlined by Jacob et al [8], for manufacturing large structures such as wind turbine blades, some of the processing requirements include low exotherm, long infusion windows and fast cure response so that process cycle times can be reduced without compromising the quality of the blade. In an attempt to meet these requirements, latent resin systems have been developed which are comparatively stable at ambient conditions but react faster when the temperature is increased [8, 9]. In the present study, heat-activated epoxy powders have been investigated as a latent resin system in low-cost VBO prepregs for thick-section composite parts (up to 120mm thick) such as the root section of a wind or tidal turbine blade.

Powdered thermosetting polymers have found widespread usage in the coating industry because they produce little or no volatile organic compounds (VOCs), offer high utilisation, and do not result in waste disposal problems [10]. Typically, the powders contain a resin, a hardener, and may contain a catalyst and other additives [11-15]. Polyester and epoxy powders are common within both the coating industry and the composites industry; however, epoxy matrices are generally favoured for wind and tidal turbine composite blades due to their superior strength and stiffness. The powders are applied to parts via electrostatic spray or another deposition process [16]. Once applied, the powder is heated to form a molten polymer coat and, at a sufficiently high temperature, the latent curing agents activate and the coating cures.

In terms of use as a polymer matrix in fibre-reinforced composite materials, one concept that was previously explored in the aerospace industry was the production of ‘towpreg’, where carbon-fibre tows were individually spread and either thermoset or thermoplastic powder was sprayed into the tow. These tows could subsequently be braided, woven, turned into tape for automated tape placement, or used to make pultruded sections [17-19]. By depositing the powder directly into the tow, the polymer was not required to flow into the tows, making the process suitable for use with thermoplastic powders. Despite this, producing a fabric or pultruded section from ‘towpreg’ required more ancillary processes such as re-spooling, lubrication of the tows prior to weaving or braiding, or pressurised die consolidation in the case of pultrusion. These additional processes added more cost and complexity to the material production. An alternative, cost-effective approach is to deposit and sinter the powder onto one or both sides of the fabric so that a VBO prepreg is formed [5]. The deposited powder must be capable of achieving low viscosity so that it can be infused into the fabric during part consolidation. Conventional thermoplastic powders are not suitable due to their high viscosities; however, the epoxy powders investigated in this study are suitable and can be used to create a VBO prepreg with a long out-life due to the stability of the epoxy powder mixture at ambient temperatures [5].

An important advantage of epoxy powders, in comparison with conventional epoxy systems, is that they produce a smaller exothermic reaction when curing, see Table 1. This is of particular interest when manufacturing thick-section structures, such as those found in wind and tidal turbine blades, because large exothermic reactions can result in damage to the final product, resulting in high scrappage rates [21, 24]. In addition, the heat-activated curing agents in the epoxy powder allow the powder to melt at elevated temperatures without inducing significant cure. Consequently, components (e.g. blade skins and spars) can be consolidated in isolation, solidified into preforms, assembled, and then co-cured to form one structure without the need for adhesive bonding. The drawback of the heat-activated curing agents is that higher temperatures are required for curing (> 160°C) than what is typical for conventional resin systems; as such, large ovens or specialised, heated tools are required for manufacturing. More recently, integrally-heated ceramic tooling was used to produce “one-shot” 12.6m wind turbine blades from glass-fibre/epoxy-powder VBO prepreps [5], as shown in Fig. 2.

**Table 1**  
Comparison of epoxy powders with some conventional epoxy systems.

<b>Resin system type</b>	<b>Total enthalpy of reaction (J/g)</b>
<b>Powder coating</b>	78.0 – 137.7 [11]
<b>Powder coating</b>	38.9 [13]
<b>Powder coating</b>	44.5 [15]
<b>Resin transfer moulding (RTM)</b>	441.0 – 469.0 [20]
<b>Resin film infusion (RFI)</b>	435.4 [21]
<b>Infusion</b>	425.3 [22]
<b>Prepreg</b>	560.0 [23]



**Fig. 2.** Ceramic heated tools (left); and 12.6 m blades made from epoxy powder based VBO prepreg (right).

This technology has the potential to fulfil the mechanical performance and cost savings required for composite components in WECs and TECs [25, 26]; however, in general, it has been identified that VBO prepregs are sensitive to variations in key process parameters and can fail to meet the required quality if the correct conditions are not met [3]. It has been shown that void formation can occur due to dissolved moisture in the resin [27], cure kinetics and viscosity can be altered by out-time effects [28], and the processing window for VBO prepreg resins tends to be smaller than conventional prepreg resins due to the former's high initial viscosity and increased reactivity at elevated temperatures [4]. As such, a greater understanding of the materials is required to develop the technology for processing thicker parts such as tidal turbine root sections and wind turbine spars [29].

The characterisation of thermosetting polymers has been well documented and detailed characterisation procedures are available [30]. Thermosetting powders, mainly epoxies and polyesters, have also been the subject of numerous characterisation studies within the coating industry. Early research focussed on the use of experimental techniques to characterise the cure and viscosity of coatings due to their importance for film formation and surface adhesion [11, 12]. Subsequent work by others [13-15] has investigated various means of modelling the cure kinetics of these thermosetting powders. Ramis et al [14] used an isoconversional kinetic analysis method to determine the mechanical and chemical curing kinetics of a polyester powder coating and to construct a time-temperature-transition (TTT) diagram. Saad et al [13] investigated what effect the presence or absence of a catalyst had on the cure kinetics of a hybrid epoxy/polyester powder coating.

In relation to fibre-reinforced composite materials, polymer powders have also been investigated as binders which help to bond individual plies of fabric together and produce a preform for subsequent resin infusion [20, 31, 32]. For these studies, the main topics of interest were the solubility of the binder in the infusion resin and the effect of binders on both the processing parameters and the mechanical properties of composite materials. Depending on the combination of binder and infusion resin, it was found that the binder could affect reaction kinetics, viscosity and interlaminar properties. Lionetto et al [20] modelled the effect of a soluble epoxy binder powder on the cure kinetics and chemorheology of an RTM-grade epoxy resin, finding that the binder had a significant effect on the cure kinetics.

Despite the prevalence of thermosetting powders for coatings and binder systems, little or no recent research has been published on their application as the primary polymer matrix in fibre-reinforced composite materials. Focussing on thermal analysis, the aim of the present work was to characterise the candidate epoxy powders and to investigate how they would perform as the primary polymer matrix during consolidation and curing of a thick-section composite part. DSC and parallel-plate rheometry were used to generate sets of experimental data for the melting and curing of the epoxy powders. The data for one epoxy powder has been fitted to models which describe the cure kinetics and chemo-rheological behaviour of the polymer with respect to time and temperature. These semi-empirical models have been applied to a typical composites processing cycle to evaluate whether the model was accurate and if the process cycle could be improved in order to reduce production time and cost. Supplementary analysis has been performed using TGA to determine the thermal stability of the epoxy powders.

## 2. Materials and methods

Two development epoxy powders were investigated; GRN 918 supplied by ÉireComposites Teo. [33], and HZH01R supplied by AkzoNobel which is a commercial epoxy resin system designed as a binder for glass fibre impregnation [34].

The epoxy powders are known to be slightly hygroscopic (approx. 0.4-0.6% moisture uptake, w.r.t. dry mass, for ambient storage conditions). For this reason, during processing the composite preform is dried under vacuum for an extended period of time. To replicate the state of the epoxy powder during VBO processing, all samples were dried under vacuum at 40°C for at least 12 hours, and were then stored in sealed jars with silica gel until testing. In all cases, test sample loading of the epoxy powder was performed in a timely manner to ensure minimum moisture uptake from the ambient air.

### 2.1. Thermal stability

Exposing thermoset resins to temperatures outside a range where they are chemically stable can significantly reduce both the glass transition temperature and the mechanical properties of the cured material due to bond scission and other chemical transformations [35]. As such, the first stage of the thermal analysis was to identify the onset of thermal degradation for the epoxy powders. Thermogravimetric analysis was used to measure the weight loss of the resin sample due to thermal decomposition. Testing was performed using a SDT-Q600 TGA/DSC to the specifications of ISO 11358-1. Samples were tested in alumina crucibles; the initial mass was  $12.5 \pm 0.25$  mg for all samples. Tests were carried out in an inert nitrogen atmosphere using a nitrogen purge gas with a flow rate of 50 ml/min. Non-isothermal tests were carried out at a ramp rate of 10°C/min between 25°C and 600°C.

### 2.2. Cure kinetics

The curing process is critical in achieving high mechanical properties for thermoset composite parts. During this process, the thermoset undergoes numerous complex chemical reactions involving polymerisation, branching and crosslinking; generating an exothermic heat flow that can be measured using DSC. In this study, a DSC Q200 (TA Instruments) was used to measure the heat flow for the epoxy powders. Testing was performed to the specifications of ISO 11357-5. All epoxy powder samples (weighing  $6.5 \pm 0.4$  mg) were loaded into ventilated aluminium crucibles. The nitrogen purge flow rate was 50 ml/min. For isothermal DSC, the samples were loaded in ambient conditions and the ramped to test temperature at 50°C/min. The isothermal tests were performed at 160°C, 170°C and 180°C. Four ramp rates were used for non-isothermal tests; ramp rates of 0.5, 1.0, and 1.5°C/min were used to determine the cure kinetics of the GRN 918 epoxy powder and 10°C/min was used to compare GRN 918 and HZH01R. A replication of a typical processing cycle was also performed on GRN 918 for comparison with the cure kinetics model.

Cure kinetics modelling may be split into two main approaches; mechanistic and phenomenological. The latter approach was used in the present study because exact formulations for the supplied epoxy powders were not available, and many semi-empirical models exist for thermosetting materials [36]. The enthalpy of the curing reaction was measured by DSC based on the exothermic heat flow from the epoxy powder at elevated temperatures. For fitting DSC data to the semi-empirical models, it was assumed that the rate of change in the enthalpic heat flow,  $dH/dt$ , was proportional to the reaction rate,  $d\alpha/dt$ :

$$\frac{d\alpha}{dt} = \frac{1}{H_T} \frac{dH}{dt} \quad (1)$$

where  $H_T$  is the total enthalpy of reaction. The degree of cure,  $\alpha$ , was determined by integrating Equation (1) with respect to time as follows:

$$\alpha = \frac{1}{H_T} \int_0^t \left( \frac{dH}{dt} \right) dt \quad (2)$$

By converting the DSC data into degree of cure data using Equations (1) and (2), it was possible to populate a semi-empirical model and determine the kinetic constants and fitting parameters which described the curing behaviour. The following  $n^{\text{th}}$  order, autocatalytic model has been established for describing the kinetics of epoxy curing reactions [37]:

$$\frac{d\alpha}{dt} = (k_1 + k_2\alpha^m)(1 - \alpha)^n \quad (3)$$

where  $m$  and  $n$  are the reaction orders, and  $k_1$  and  $k_2$  are the rate constants which have a temperature dependency described by the following Arrhenius expression:

$$k_i = A_i \exp\left(\frac{-E_i}{RT}\right) \quad (4)$$

where  $A$  is pre-exponential constant,  $E$  is the activation energy,  $R$  is the universal gas constant, and  $T$  is temperature in Kelvin.

Based on non-isothermal DSC traces of the epoxy powder at low ramp rates ( $< 1.5^\circ\text{C}/\text{min}$ ), it was assumed that the curing agents did not activate below  $120^\circ\text{C}$  approximately (see supplementary data). Above and below this activation temperature, the reaction rate displayed different temperature dependencies such that Equation (3) could not sufficiently describe the cure kinetics for both low and high temperatures. To account for this behaviour, a third rate constant, for cure at lower temperatures, was added to Equation (3) as follows:

$$\frac{d\alpha}{dt} = (k_1 + k_2 + k_3\alpha^m)(1 - \alpha)^n \quad (5)$$

The accuracy of the  $n^{\text{th}}$  order, autocatalytic model was improved at higher conversion levels by accounting for the transition to a diffusion-controlled reaction [38], as follows:

$$\frac{d\alpha}{dt} = \frac{(k_1 + k_2 + k_3\alpha^m)(1 - \alpha)^n}{1 + \exp[C(\alpha - \alpha_c(T))]} \quad (6)$$

where  $C$  is the diffusion control factor and  $\alpha_c(T)$  is the temperature-dependent critical degree of cure above which the reaction becomes diffusion-controlled.

The cure kinetics model was used to predict the glass transition temperature,  $T_g$ , of the resin for a given process cycle. To be able to make this prediction, additional DSC testing was required to determine the relationship between degree of cure and  $T_g$ . For the additional tests, epoxy powder samples were partially cured isothermally at  $160^\circ\text{C}$  and then re-heated, using a dynamic run at a heating rate of  $1.5^\circ\text{C}/\text{min}$ , to determine the new glass transition temperature and the residual enthalpy of reaction. In this case, where the relationship was non-linear, the DiBenedetto equation was found to be suitable [39]:

$$\frac{T_g - T_{g0}}{T_{g\infty} - T_{g0}} = \frac{\lambda\alpha}{1 - (1 - \lambda)\alpha} \quad (7)$$

where  $T_{g0}$  is the initial glass transition temperature of the uncured resin,  $T_{g\infty}$  is the glass transition temperature of the fully cured resin, and  $\lambda$  is fitting constant.

### 2.3. Chemorheology

As previously mentioned, VBO prepregs are only partially impregnated with the resin matrix, so that the dry fibre pathways can evacuate air and vaporised moisture. Centea et al [3] outlined that the resin must be sufficiently resistant to flow at lower temperatures so that these airways remain open, while at the same time the resin must achieve a low enough viscosity at elevated temperatures to flow into the dry fibre tow and achieve full consolidation of the final part.

The chemorheological behaviour of the epoxy powders was characterised using an AR 2000ex rheometer (TA Instruments), with an environmental test chamber. Aluminium parallel plates with a diameter of 25 mm were used. Testing was performed in oscillation mode to the specifications of ISO 6721-10. In all cases, samples weighing 900 mg were loaded in powder form at ambient temperature with the aid of a melt ring. The sample was brought to 100°C to allow it to become molten before the gap was reduced to 1000 microns and excess resin was removed. The environmental test chamber used forced air convection for heating with an air flow rate of 20 l/min. Initially, strain sweeps and frequency sweeps were performed at temperatures between 50°C and 120°C in order to choose test parameters that would remain within the linear viscoelastic region (LVR). A strain of 1% and a frequency of 5 rad/s were chosen, and all tests began from 70°C in order to capture the rheological behaviour of the epoxy from lower temperatures while staying within the LVR. Isothermal tests were performed at 150°C, 160°C and 170°C so that the viscosity rise due to curing could be measured. Curing of the epoxy began immediately at these temperatures. To account for this rapid curing, the test samples were heated as quickly as possible to test temperature while minimising overshoot; the latter was kept to 3°C or less for all tests, with equilibrium typically achieved within 30 seconds. In the case of non-isothermal tests, ramp rates of 5°C/min and 10°C/min were used (tests began at 70°C and continued to rise in temperature until gelation). Similar to the DSC testing, a replication of a typical processing cycle was performed on GRN 918 for comparison against the chemorheological model.

Chemorheological models account for the viscosity change in a polymer system as it cures; for this reason, the cure kinetics model was implemented as a sub-model which predicted cure progression. The Castro-Macosko model, originally developed for polyurethanes [40] but widely used for thermosetting resins [21, 41], was previously investigated for use with epoxy powders [42]. It was found that the Arrhenius expression (used in the model for describing the viscosity before cure) did not correspond well with the behaviour of the epoxy powder. A similar problem was encountered by Kenny and Opalicki [23] who developed the following model for toughened epoxies:

$$\eta = \eta_{g0} \exp\left(\frac{-C_1[T - T_g(\alpha)]}{C_2 + T - T_g(\alpha)}\right) \left(\frac{\alpha_g}{\alpha_g - \alpha}\right)^n \quad (8)$$

where  $\eta_{g0}$  is the unreacted resin viscosity at the initial glass transition temperature,  $T_{g0}$ ,  $\alpha_g$  is the degree of cure at the gel point, and  $C_1$ ,  $C_2$ , and  $n$  are fitting constants. Kenny and Opalicki used the classical Fox equation, from glass transition theory, to describe a linear relationship between the glass transition temperature and the degree of cure. In the case of GRN 918, Equation 7 was used to fit the experimental data instead of the Fox equation because the relationship became non-linear after gelation.



### 3. Results and discussion

#### 3.1. Thermal stability

Manufacturing thick-section composite parts with thermosetting resins is challenging due to the combination of the exothermic heat flow from the curing reaction and the poor thermal conductivity of the composite itself; especially in the case of glass-fibre reinforcement. For resin systems with large exotherms ( $> 400$  J/g), processing is limited by how quickly heat can be transferred out of the composite. Using ramp rates that are too fast can lead to “thermal runaway” of the material i.e. a loss of control over the curing reaction. The risk should be reduced for resin systems with smaller exotherms; however, significant temperature gradients can still develop when transferring heat into the material due to its insulative properties in the out-of-plane direction. Large temperature gradients may subsequently result in the development of locked-in residual stresses and warpage [22, 43]. In the more extreme case of “thermal runaway”, if high enough temperatures are reached during processing, the resin will become unstable and begin to decompose, resulting in severely reduced mechanical properties [35].

Focussing on the latter case, TGA was used to determine an upper limit for processing the thermosetting resin. Fig. 3 shows that the onset of decomposition for the epoxy powders occurred above  $350^{\circ}\text{C}$ , a much higher temperature than the typical processing range (i.e.  $140 - 210^{\circ}\text{C}$  for curing). Furthermore, as discussed in subsequent section, the risk of “thermal runaway” is lessened by the fact that the epoxy powders generated relatively small exotherms upon curing.

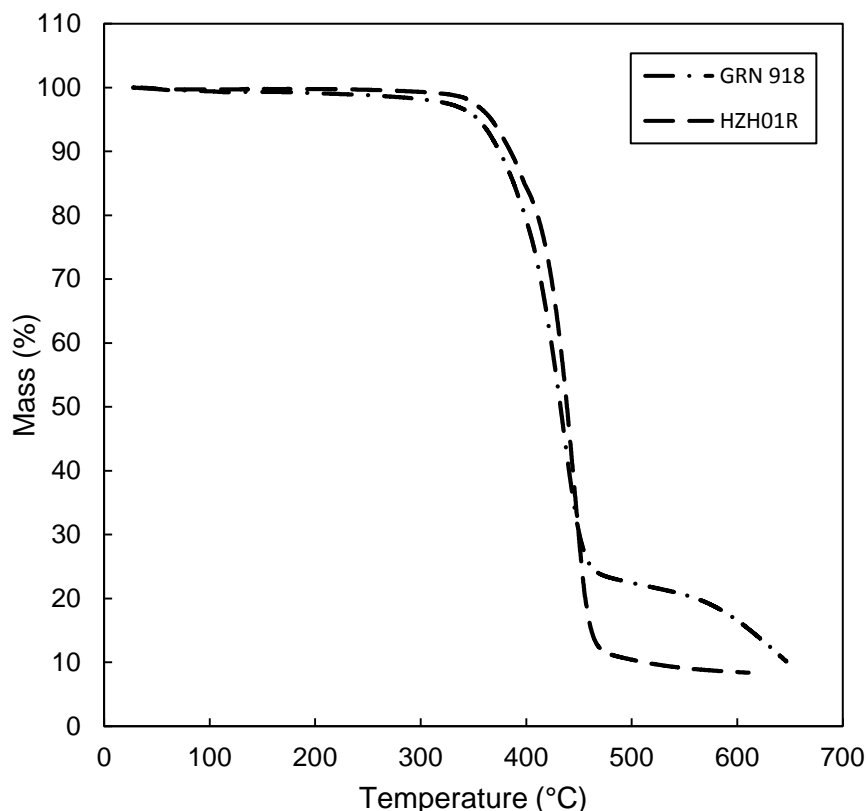


**Fig. 3.** Mass loss due to thermal decomposition of the epoxy powders. Temperature was increased at  $10^{\circ}\text{C}/\text{min}$ .

### 3.2. Cure kinetics

In general, VBO prepreg resins must be formulated with sufficient chemical stability to lay-up the composite laminate and vacuum bagging materials at ambient conditions, and evacuate any air or vaporised moisture. Consequently, elevated temperatures are required to cure these resins fully.

The DSC traces in Fig. 4 show that both epoxy powders exhibited good characteristics for VBO prepreg processing. At ambient conditions, the powders maintained a glassy state because they were below their glass transition temperature. This meant that the molecular mobility of the resin was low and cure could only occur via a diffusion-controlled mechanism. As a result, the powders had a long out-life when compared to conventional prepreg resins which often must be refrigerated to suppress the curing reaction. In the case of HZH01R, the storage stability at ambient conditions was up to 4 months from the date of manufacture [34].

To create a VBO prepreg with the epoxy powders, the powder must be calendared onto one or two sides of dry fabric at a slightly elevated temperature such that the powder can effectively sinter together with the dry fabric. By only sintering the powder, the VBO prepreg can retain some drapability and the sintered powder forms an additional flow path through which trapped air and vaporised moisture can be evacuated.

The transition from loose powder to a highly viscous liquid was identified by two overlapping events; enthalpic relaxation (endothermic peak) and glass transition step change in heat flow. At temperatures above this transition, the resin began to react; however, any resulting exotherm was difficult to measure because the reaction rate was slow. In contrast to this, the catalysed curing reaction generated an exothermic peak in the heat flow data above 150°C. For both resin systems, the total enthalpies of reaction (184 J/g for GRN 918 and 138 J/g for HZH01R) were small when compared to other epoxy resin systems which can produce greater than 400 J/g [20-23]. This is advantageous for manufacturing thick-section parts where large enthalpies can make reactions and thermal gradients difficult to control, as previously discussed. For HZH01R, both the transition from powder to liquid and the onset of cure occurred at higher temperatures than GRN 918, suggesting that it may have had better stability in warmer storage conditions without requiring a significantly higher curing temperature.

The characteristic values for the DSC traces are given in Table 2; it should be noted that these characteristic values were rate-dependent and 10°C/min was chosen for comparative purposes because higher ramp rates gave greater resolution for the differences between the powders.

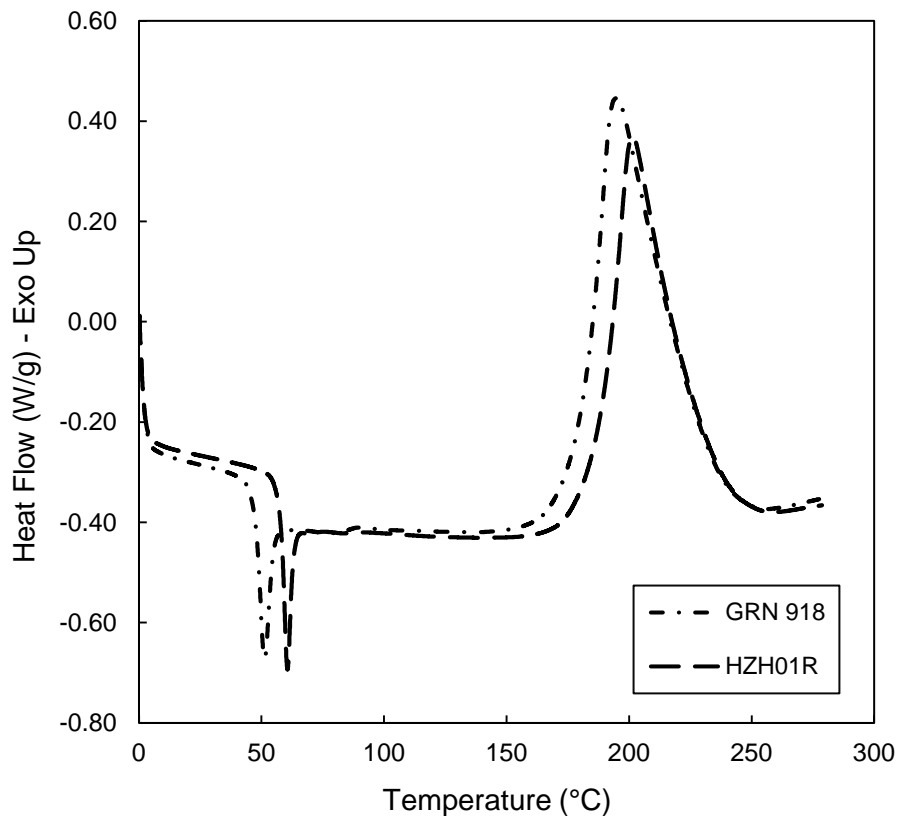


**Fig. 4.** DSC traces for both epoxy powders at a heating ramp rate of 10°C/min. Note, positive exothermic heat flow.

**Table 2**

Non-isothermal DSC measurements for the epoxy powders at a heating ramp rate of 10°C/min.

Characteristics	GRN 918	HZH01R
Enthalpic relaxation onset temperature (°C)	47.6	57.7
Enthalpic relaxation peak temperature (°C)	51.4	60.5
Curing onset temperature (°C)	180.1	186.7
Curing peak temperature (°C)	194.8	201.2
Max total enthalpy of reaction (J/g)	184.0	138.0

For cure kinetics modelling, GRN 918 was used as a case study. The isothermal DSC data, shown in Fig. 5, was integrated according to Equation 2. Equation 6 was then fitted to the resulting degree of cure curves using MATLAB's in-built nonlinear least-squares curve fitting capabilities. A more accurate value for the rate constant,  $k_1$ , was determined by fitting to non-isothermal DSC data with slower temperature ramp rates (i.e. 0.5 – 1.5°C/min); this allowed time for a small amount of uncatalysed reaction to develop. The parameters for Equation 6 are given in Table 3. Note that the critical degree of cure was temperature-dependent. The isothermal DSC data shows that the catalysed cure time for the epoxy powder changed considerably for 10°C increases in temperature. This behaviour was reflected in the activation energies and pre-exponential constants for the catalysed reaction, which were much larger than what is typically reported for epoxy resins [13, 20-23, 30]. Most likely this was due to the effects of the curing agents which, once activated, caused the

temperature-dependency of the reaction rate to change significantly; hence, the need for an additional rate constant to accurately model the cure kinetics at lower temperatures.

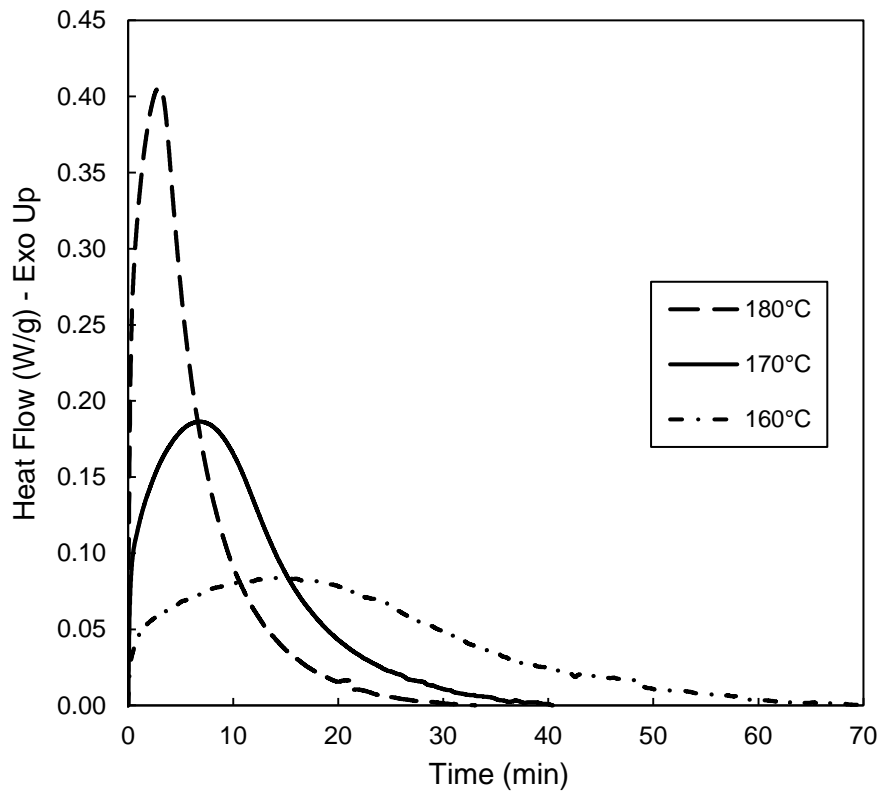


Fig. 5. Isothermal DSC traces for GRN 918.

**Table 3**  
Cure kinetics model parameters for GRN 918.

Parameter [unit]	Value	Parameter [unit]	Value
$A_1$ [ $s^{-1}$ ]	$4.073 \times 10^{-4}$	$m$	1.24
$E_1$ [J/mol]	12006	$n$	1.8
$A_2$ [ $s^{-1}$ ]	$10.112 \times 10^9$	$C$	50
$E_2$ [J/mol]	111792	$\alpha_c(T)$	$0.006 T - 1.748$
$A_3$ [ $s^{-1}$ ]	$1.636 \times 10^{13}$		
$E_3$ [J/mol]	131240		

Fig. 6 and Fig. 7 display how the cure kinetics model compared to the experimental DSC data. In general, there was good agreement between the model and the data. For isothermal conditions, the model was accurate in accounting for the transition to diffusion-controlled cure. The effect of the additional rate constant,  $k_1$ , was more evident for the  $1.5^\circ\text{C}/\text{min}$  non-isothermal test (i.e. approximately 5% conversion happened below  $120^\circ\text{C}$ ). Although this small amount of cure may seem inconsequential, manufacturing thick-section parts using VBO prepregs requires slow ramp rates and long dwell periods to allow the material to fully consolidate. In this sense, it was useful to evaluate the model based on an actual processing cycle for a thick-section composite part. This processing cycle involved the following stages:

- Stage 1: The epoxy resin was heated from ambient temperature to 120°C at a rate of 1.5°C/min, and then allowed to dwell isothermally so that it could flow and infiltrate the reinforcing fabric under vacuum pressure.
- Stage 2: The resin was cooled back down to ambient conditions so that it would solidify and create a fully consolidated preform.
- Stage 3: The various preforms were assembled together and re-heated to 120°C so that the resin could re-melt and join at the interface of the assembled parts.
- Stage 4: The assembled components were co-cured at 180°C to form a final part.

Fig. 8 shows the cure kinetics model prediction for the above processing cycle. The model predicted that 24% conversion would be reached by the end of stage 3. This suggests that after assembly, the resin would be in a sufficiently low state of cure that individual preforms could be fused, provided that there was complete contact between them. To validate this degree-of-cure prediction, the cycle was replicated in a DSC experiment. Although, it was difficult to accurately measure the heat flow due to curing at and below 120°C, the residual enthalpy of reaction for stage 4 was measured as being 142 J/g (i.e. the epoxy had already reached 22.8% conversion by the end of stage 3). When modelling the same process cycle without the additional rate constant, only 12.1% conversion was predicted. This demonstrated that an additional rate constant was effective in improving the model's accuracy at lower temperatures. Despite this, the model could be further improved by additional testing of conditioned epoxy samples. By storing the epoxies above their glass transition temperature in a vacuum oven and then testing them periodically, it may be possible to better characterise the material's reaction kinetics at lower temperatures.

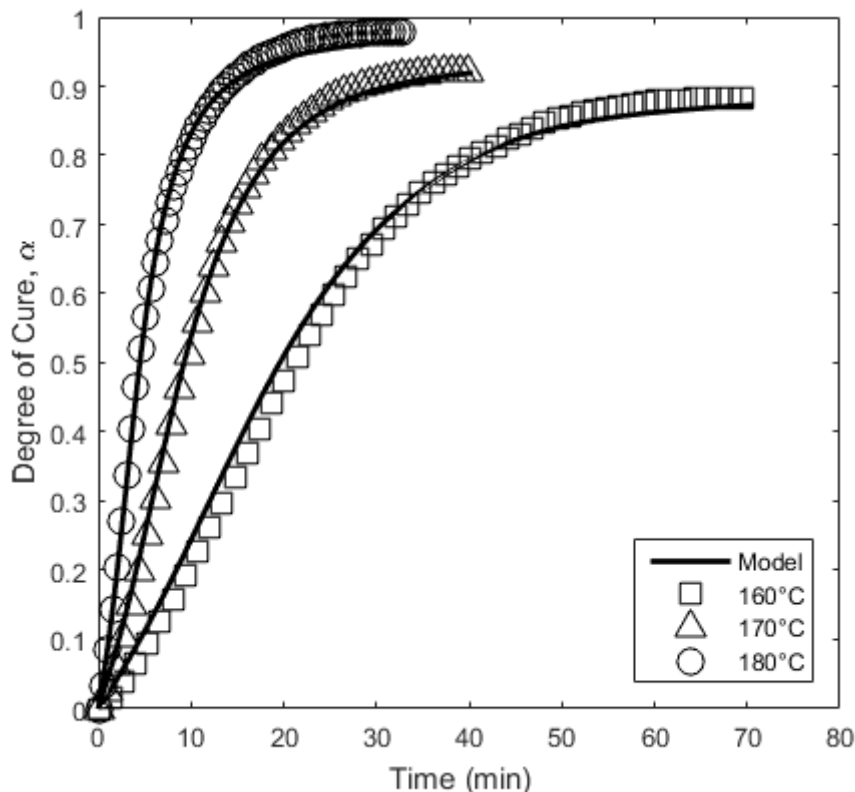


Fig. 6. Comparison of the cure kinetics model prediction and the isothermal degree of cure data for GRN 918.

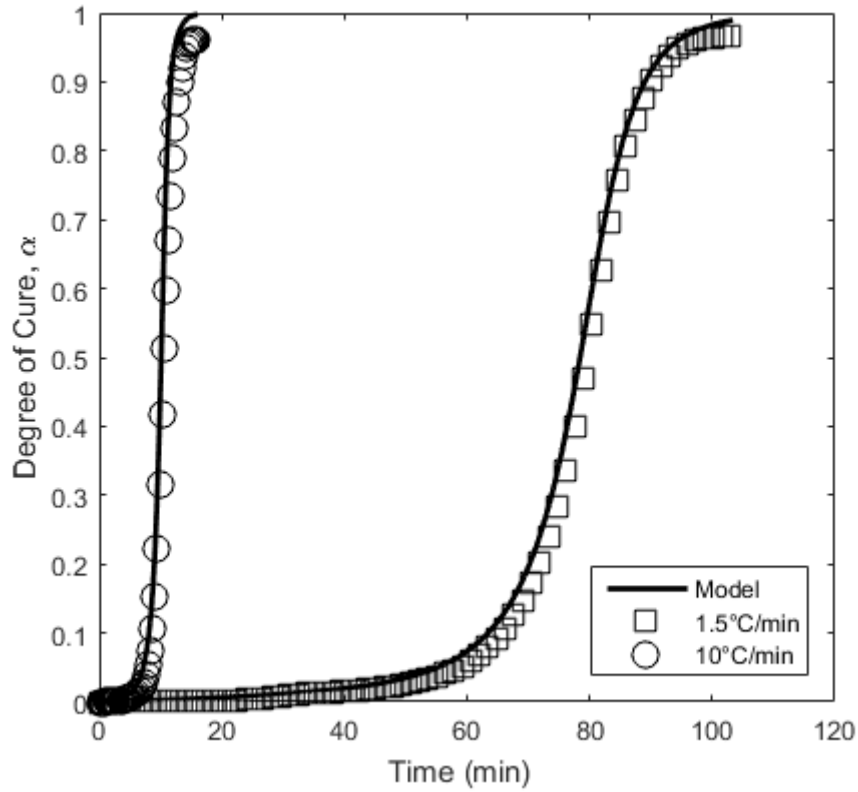


Fig. 7. Comparison of the cure kinetics model prediction and the non-isothermal degree of cure data for GRN 918.

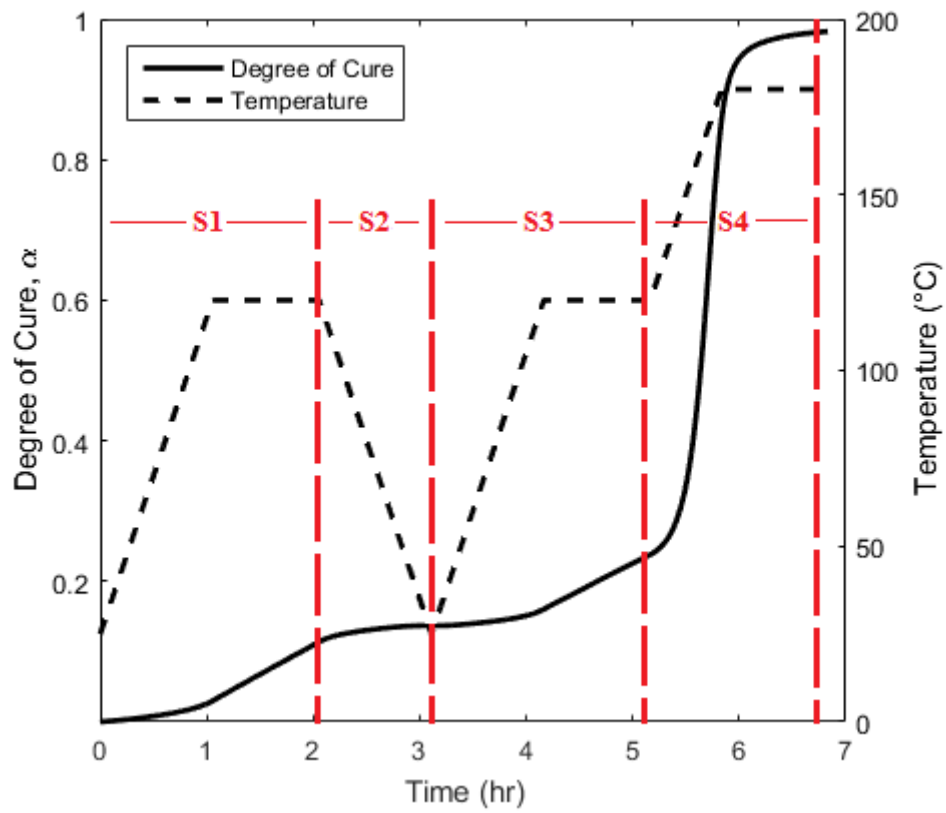
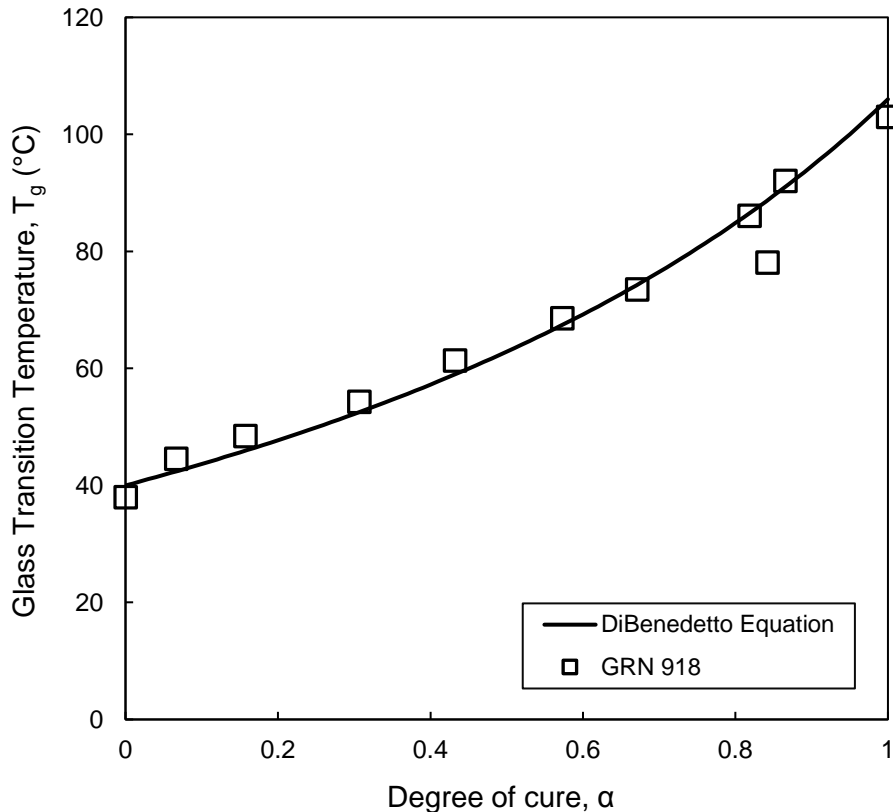


Fig. 8. Degree of cure prediction of epoxy powder (GRN 918) for a realistic process cycle. The stages of the process cycle are illustrated (S1 is Stage 1, etc.)

Additional DSC tests were carried out to determine the relationship between the glass transition temperature and degree of cure. Samples were partially cured isothermally and then a non-isothermal ramp at 1.5°C/min was used to determine the corresponding  $T_g$  onset, as well as the residual enthalpy of reaction. The initial glass transition temperature,  $T_{g0}$ , and the final glass transition temperature,  $T_{g\infty}$ , were determined using a heating rate of 1.5°C/min on uncured powder. The experimental data and the fit to the DiBenedetto equation are shown in Fig. 9. The fitting parameter,  $\lambda$ , was given a value of 0.53. The data shows that the relationship became non-linear after gelation had occurred.



**Fig. 9.** Relationship between glass transition temperature and degree of cure for GRN 918.

### 3.3. Chemorheology

During the processing of an epoxy powder based VBO prepreg, void formation due to trapped gases can be avoided by ensuring air and vaporised moisture are evacuated from the VBO prepreg below the glass transition temperature of the epoxy. By maintaining a temperature below the glass transition, the dry fibre pathways remain open and the porous powder layer can also allow for the evacuation of gases. While this presents a valuable processing advantage, it is still necessary that a VBO resin can achieve and maintain a suitably low viscosity (< 100 Pa.s) so that resin can flow into and fill the dry fabric [4].

Resin flow in fibrous materials has been widely researched due to its importance for part quality and manufacturing time. In the case of VBO prepreps, the flow is on a small length-scale when compared to processes like RTM and VIP, and can be governed by Darcy's Law for flow through a porous medium [44, 45]. The resin must flow into the individual fibre tows which can have a permeability that is one or two orders of magnitude lower than the bulk fabric [46]; making the resin viscosity a key parameter in the consolidation process.

Using parallel-plate rheometry, the viscosities of the two melted epoxy powders were measured for non-isothermal conditions; the comparison is shown in Fig. 10. While DSC data showed that the powder-to-liquid transition was between 40°C and 60°C, the resin viscosity did not enter a suitable range for processing below 100°C. The epoxies displayed similar behaviour to each other; however, the GRN 918 epoxy achieved the required processing viscosities over a wider range of temperatures, giving it greater flexibility for consolidating thick laminates. For a ramp rate of 5°C/min, minimum viscosities of 1 Pa.s and 2.3 Pa.s were measured for GRN 918 and HZH01R, respectively.

In terms of the chemorheological modelling, it should be noted that viscosity curves for both epoxy powders in Fig. 10 did not follow an Arrhenius temperature-dependency as is required to fit the Castro-Macosko model. From the non-isothermal DSC data for GRN 918, it was evident that the reaction rate of the epoxy was dependent on the temperature ramp rate; however, Fig. 11 shows that the initial viscosity curve was *not* dependent on the temperature ramp rate. From this, it can be inferred that this initial viscosity behaviour was not the result of curing.

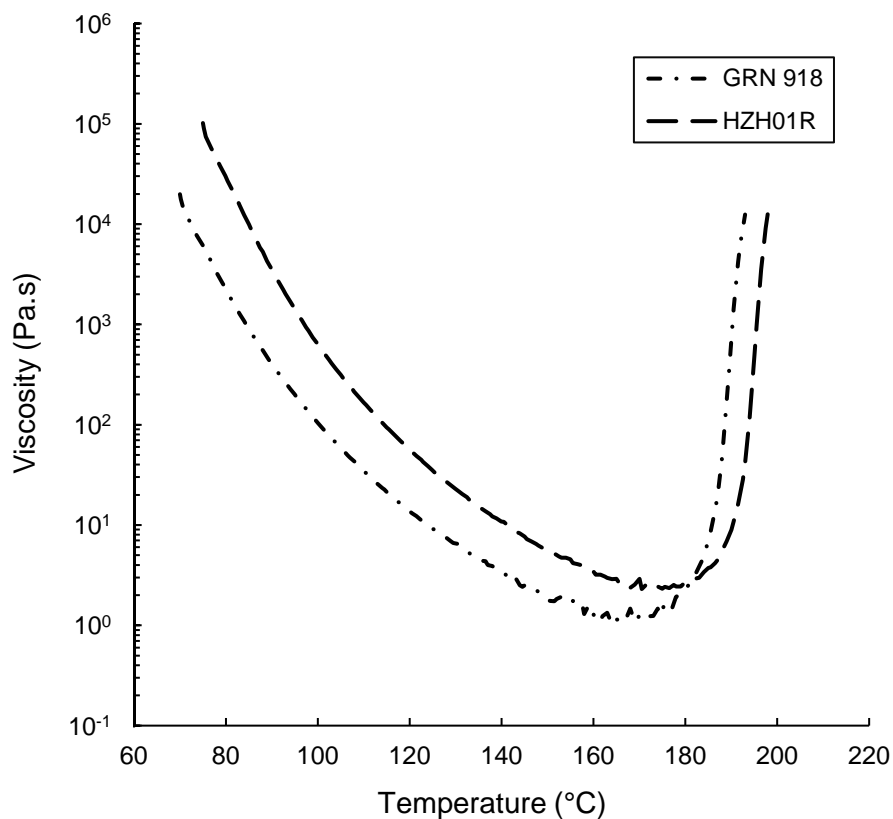


**Fig. 10.** Viscosity curves for both epoxy powders. Temperature was increased at 5°C/min.



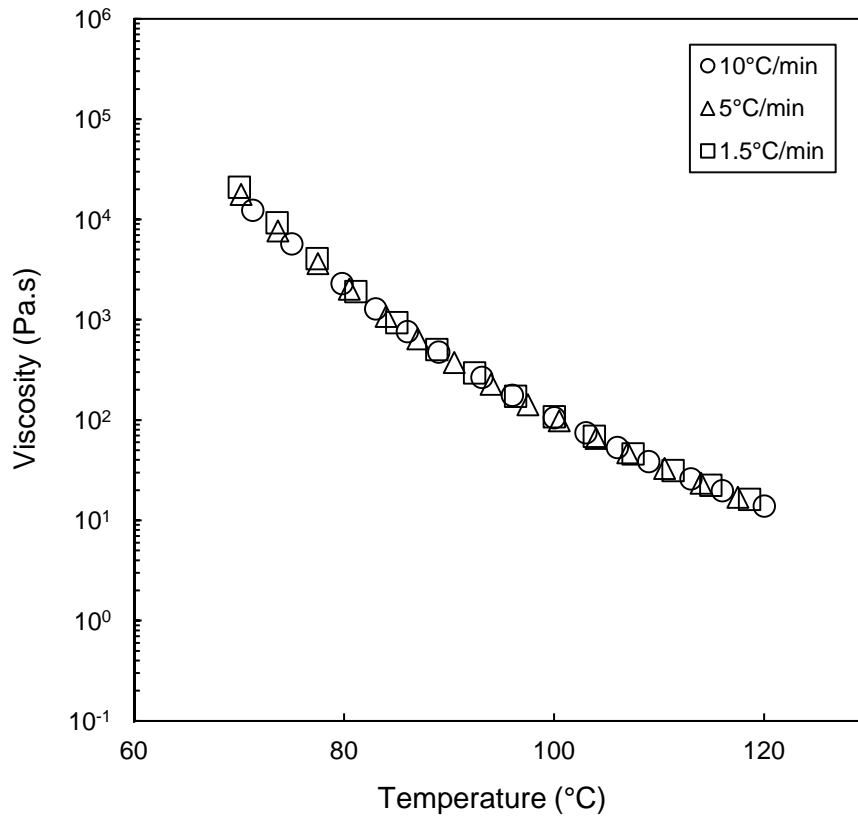
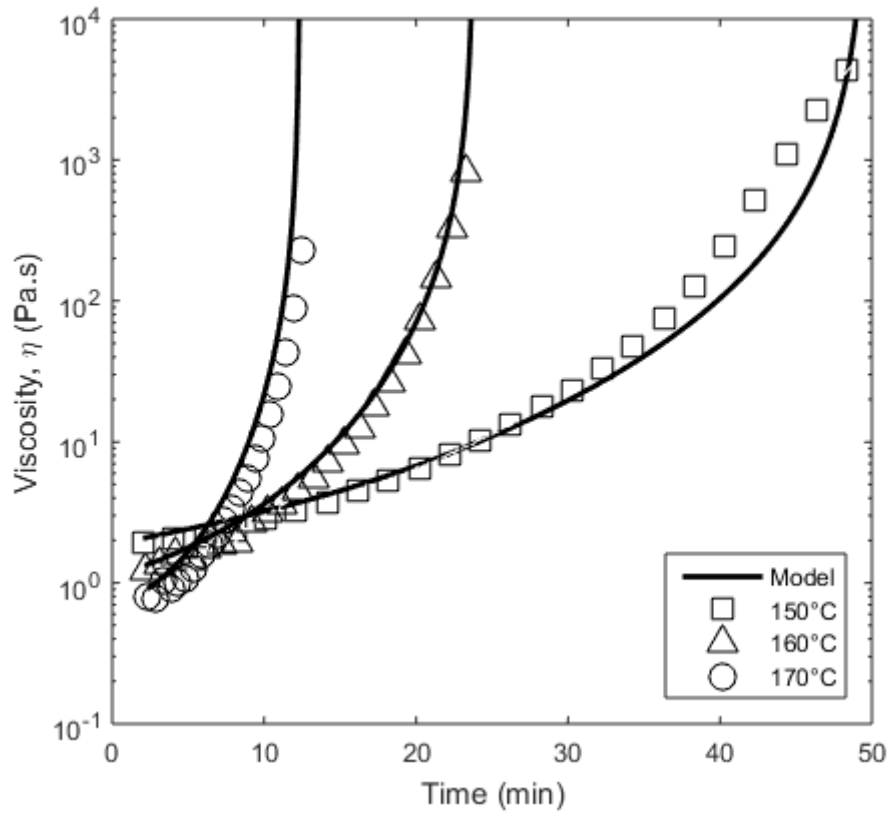


Fig. 11. Initial viscosity curves for GRN 918 at various temperature ramp rates.

Once again, GRN 918 was used as a case study for chemorheological modelling of the epoxy powders. The fitting parameters of the exponential term in Equation 8,  $C_1$  and  $C_2$ , along with the unreacted resin viscosity,  $\eta_{g0}$ , at the initial glass transition temperature were fitted to the non-isothermal data shown in Fig. 11. The degree of cure at gelation,  $\alpha_g$ , was determined using the crossover in storage and loss moduli data measured with the rheometer (see supplementary data). The remaining fitting parameter,  $n$ , was fitted to isothermal rheology data which reflected the viscosity rise due to curing. The values of all the parameters used in the chemorheological model are given in Table 4.

**Table 4**  
Chemorheological model parameters for GRN 918.

Parameter	Value	Parameter	Value
$\eta_{g0}$ (Pa.s)	$2 \times 10^{11}$	$\alpha_g$	0.56
$C_1$	32.25	$n$	1.6
$C_2$	30		



**Fig. 12.** Comparison of the chemorheological model prediction and the isothermal viscosity data for GRN 918.

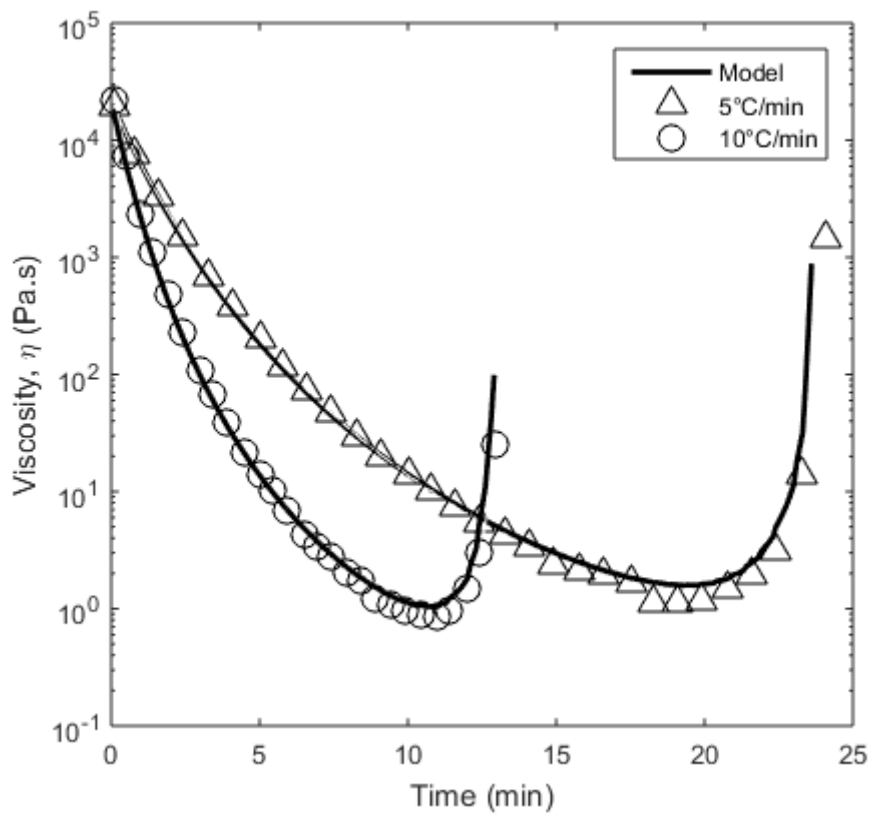


**Fig. 13.** Comparison of the chemorheological model prediction and the non-isothermal viscosity data for GRN 918.

Comparisons of the chemorheological model and experimental data for isothermal and non-isothermal conditions are shown in Fig. 12 and Fig 13, respectively. The model accurately described the behaviour of the epoxy prior to the initiation of catalysed curing, which was previously not possible with the Castro-Macosko model. For both isothermal and non-isothermal conditions, the model also provided an adequate fit for the viscosity rise due to cure.

Kratz et al [4] developed cure kinetics and chemorheological models for two VBO prepreg resins (Cycom 5320-1, ACG MTM45-1) and compared them against an autoclave prepreg resin (HexPly 8552) to investigate the difference in processing characteristics. Implementing the same models for isothermal dwells at 121°C, Centea et al [3] found that the VBO resins could not maintain low viscosities (< 100 Pa.s) for as long as the autoclave resin. This was due to the higher reactivity of the VBO resins. The model predictions, in Fig. 14, showed that this is not necessarily the case for GRN 918, which was less reactive at lower temperatures; it would take over 8 hr at 121°C to reach gelation (i.e. 56% conversion). As a result, the GRN 918 powder could maintain a viscosity below 100 Pa.s for 300 min, approximately 200 min longer than Cycom 5320-1 and ACG MTM45-1. This was longer than even the autoclave resin at the same processing temperature; however, as demonstrated originally by Kratz et al, the Hexply 8552 resin can maintain a viscosity below 100 Pa.s for almost 600 min at 90°C, which was not possible for the epoxy powder.

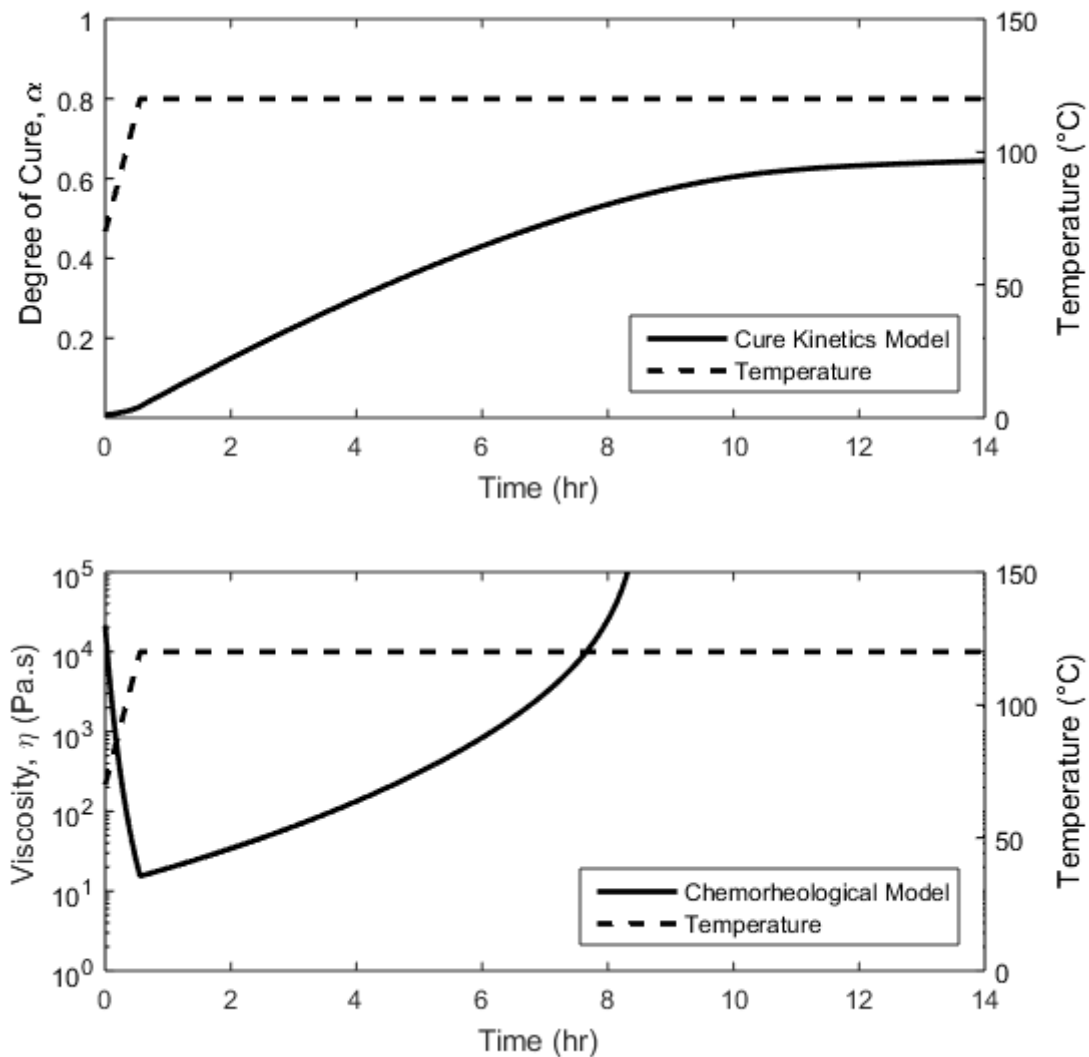


Fig. 14. Comparison of the degree of cure and viscosity for GRN 918 when held isothermally at 121°C.

Having a wider processing window is beneficial for manufacturing thick-section parts because it means that process-related defects, such as unfilled dry fabric, are less likely to occur. At the same time, to be cost-effective, the process cycle time should be optimised so that the time spent at elevated temperatures is reduced.

The process cycle, as described in the previous section, was compared with the chemorheological model. As shown in Fig. 15, the results of the model were in close agreement with the experimental rheology data. The results also showed that cure at 120°C caused a viscosity rise of 54 Pa.s during the two dwell periods. This corresponds to a 370% increase in viscosity from its initial value at 120°C. In a practical sense, most of the consolidation is expected to occur during the first dwell. Achieving low viscosities for the second dwell is not critical as individual components are only required to achieve contact so that chemical crosslinking can take place, fusing the components into a final part. For this reason, it may be possible to reduce the second dwell without adversely affecting the quality of the final part.

While it is possible to evaluate the process cycle for a small resin sample, as was the case with DSC and rheology, the process conditions throughout a thick section are inherently non-uniform because heat transfer through the thickness of the prepreg plies is slow. This means that, at various stages of the process cycle, there will be viscosity gradients and cure gradients throughout the part. As such, the resin behaviour in Fig. 8 and Fig. 15 will not fully represent the response of the whole composite laminate. Instead, the cure kinetics model and chemorheological model should be implemented in a process simulation [29]. Process simulations of an actual thick-section part, such as the root section of a wind or tidal turbine blade, would allow for better optimisation of the process cycle.

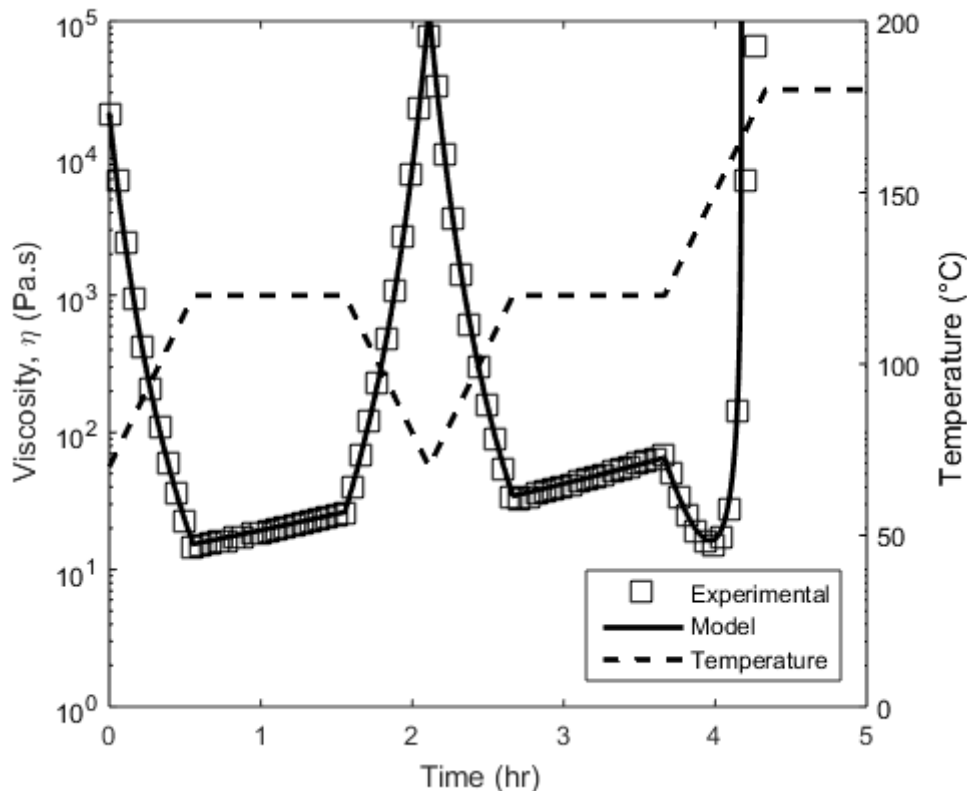


Fig. 15. Comparison of the chemorheological model prediction and the non-isothermal viscosity data for GRN 918.

#### **4. Conclusions and Future Work**

Two heat-activated epoxy powders have been characterised using thermal analysis techniques. Due to the presence of latent curing agents in the epoxy powder mixes, it was possible to store the epoxy powders in a glassy state at ambient conditions; which gave them a long out-life and made them suitable for air and moisture evacuation. The results showed that the powders could be melted to achieve low viscosities for fibre tow impregnation without inducing gelation, and subsequently re-solidified by returning to ambient temperatures. This feature meant that parts could be fully or partially consolidated in one stage, and then assembled and fused together in a separate stage to produce “one-shot” parts without any requirement for adhesive bonding. Upon curing, it has been shown that the epoxy produced a smaller exothermic heat flow compared to many epoxy systems designed for composite production. The epoxy powders were also shown to have good thermal stability, meaning that processing at high temperatures should not thermally degrade the material.

DSC data for one of the investigated epoxy powders was used to develop a modified cure kinetics model that could more accurately describe the curing behaviour of the epoxy at both high and low temperatures. An existing chemorheological model was used to describe the rheological behaviour of the same epoxy powder. The models provided good fits for epoxy powder over a wide range of processing temperatures, and could predict the epoxy powder’s behaviour for a typical processing cycle. The models were used to show that the epoxy powder met some of the key requirements for manufacturing thick-section structures. These requirements included low viscosity and low reactivity for infusion, and low exotherm and higher reactivity at elevated temperatures for curing.

Being able to model the material characteristics in this way lends itself to more advanced heat transfer and resin flow models for process simulation. Process simulations will be particularly useful for manufacturing thick-section parts where heat must be given sufficient time to transfer through the thickness of the composite plies. Such manufacturing techniques may give rise to large thermal gradients if not properly controlled, resulting in unfilled dry fabric or residual stresses within the composite material. As such, the implementation of cure kinetics and chemorheological models within larger process simulations may be used to identify an efficient processing window, so that the time and cost of manufacturing can be kept to a minimum while maintaining the quality of finished parts. Combined with mechanical test data for both dry and immersed conditions, it should be possible to fully characterise candidate materials and determine their suitability for low cost thick-section parts such as those required in wind energy and marine renewable energy applications.

#### **Acknowledgments**

The authors gratefully acknowledge financial support from MARINCOMP, Novel Composite Materials & Processes for Marine Renewable Energy, a Marie Curie FP7 Project funded under the IAPP call (Grant No. 612531), the Institute of Materials and Processes at the University of Edinburgh, industrial partners SE Blades Technology B.V., Johns Manville, MAFIC and ÉireComposites Teo. We also acknowledge funding from POWDERBLADE, Commercialisation of Advanced Composite Material Technology: Carbon-Glass Hybrid in Powder Epoxy for Large Wind Turbine Blades, Funded under: Horizon 2020, Fast Track to Innovation Pilot, Project reference: 730747. Ananda Roy at the University of Limerick and Dr. Alistair McIlhagger and Simon Hodge at Ulster University are acknowledged for their technical assistance.

#### **Appendix A. Supplementary data**

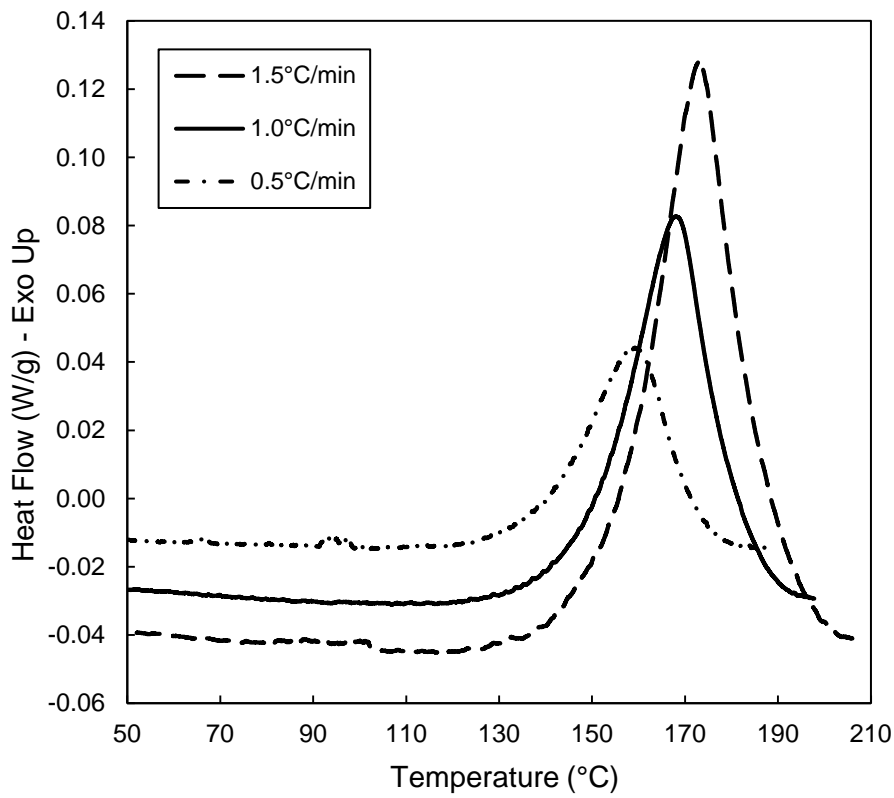


Fig. A1. Non-isothermal DSC for GRN 918 at three heating rates.

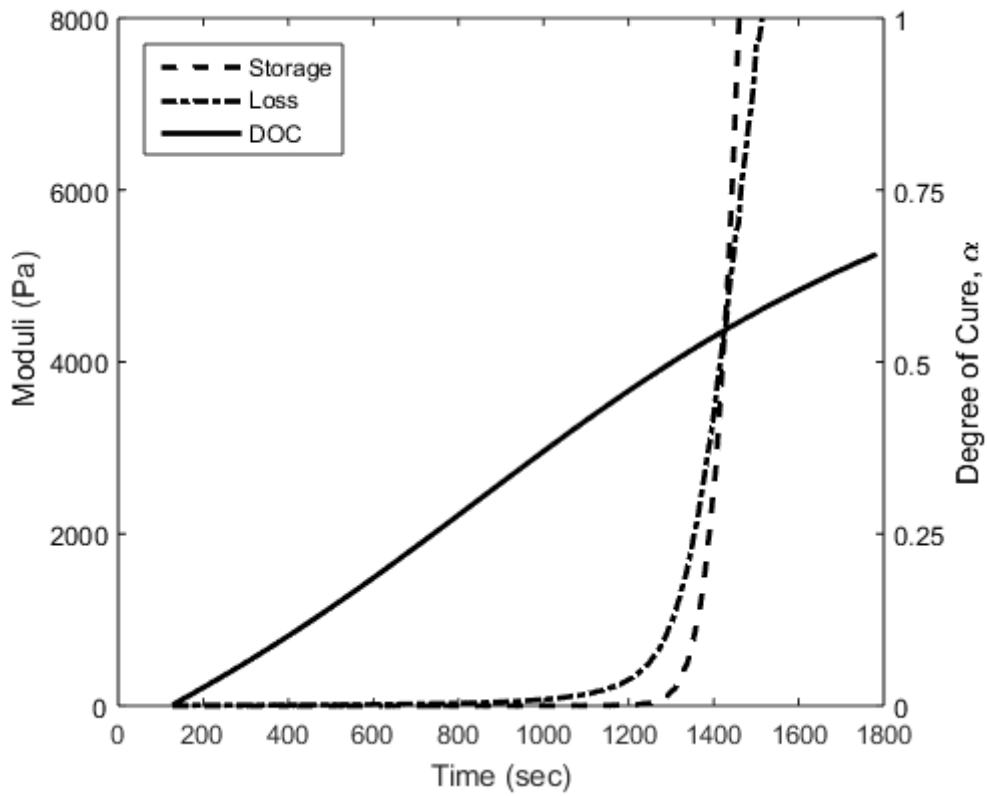


Fig. A2. The DOC at gelation for GRN 918; determined using the crossover in storage and loss moduli.

## References

1. Gardiner, G. (2015) 'HP-RTM on the rise', *CompositesWorld*, Available at: <http://www.compositesworld.com/articles/hp-rtm-on-the-rise> (Accessed: 24<sup>th</sup> January 2017).
2. Jansen, R. (2010) 'Wind energy and vacuum infusion', *Reinforced Plastics*, Available at: <http://www.materialstoday.com/composite-applications/features/wind-energy-and-vacuum-infusion/> (Accessed: 24<sup>th</sup> January 2017)
3. Centea, T., Grunenfelder, L.K., Nutt, S.R. (2015) 'A review of out-of-autoclave prepregs – Material properties, process phenomena, and manufacturing considerations', *Composites: Part A*, 70, pp. 132-154. DOI: <https://doi.org/10.1016/j.compositesa.2014.09.029>
4. Kratz, J., Hsiao, K., Fernlund, G., Hubert, P. (2012) 'Thermal models for MTM45-1 and Cycom 5320 out-of-autoclave prepreg resins', *Journal of Composite Materials*, 47(3), pp. 341-352. DOI: <http://doi.org/10.1177/00219983124440131>
5. Ó Brádaigh, C.M., Doyle, A., Doyle, D., Feerick P.J. (2011) 'Electrically-heated ceramic composite tooling for out-of-autoclave manufacturing of large composite structures', *SAMPE Journal*, 47(4) pp. 6-14.
6. Juska, T.D., Musser, B.S., Jordan, B.P., Hall, J.C. (2009) 'The new infusion: Oven vacuum bag prepreg fabrication', *Proceedings of SAMPE 2009 conference*, Baltimore MD, USA, 18<sup>th</sup> - 21<sup>st</sup> May. Society for the Advancement of Material and Process Engineering.
7. Ó Brádaigh, C.M., Grant, S., Jury, J., Naylor, D., Shanks, J. and Stratford, T. (2016) Wave Energy Scotland Materials Landscaping Study, June 2016.
8. Jacob, G.C., Hoevel, B., Pham, H.Q., Dettloff, M.L., Verghese, N.E., Turakhia, R.H., Hunter, G., Mandell, J.F., Samborsky, D. (2009) 'Technical advances in epoxy technology for wind turbine blade composite fabrication', *Proceedings of 41<sup>st</sup> International SAMPE Technical Conference*, Wichita KA, USA, 19<sup>th</sup> - 22<sup>nd</sup> October. Society for the Advancement of Material and Process Engineering.
9. Daun, G. (2009), 'Hardeners "with a switch" improve rotor production', *Kunststoffe international*, 7, pp. 54-56.
10. Misev, T.A., van der Linde, R. (1998) 'Powder coatings technology: new developments at the turn of the century', *Progress in Organic Coatings*, 34(1-4), pp. 160-168. DOI: [http://doi.org/10.1016/S0300-9440\(98\)00029-0](http://doi.org/10.1016/S0300-9440(98)00029-0)
11. Osterhold, M., Niggemann, F. (1998) 'Viscosity-temperature behaviour of powder coatings', *Progress in Organic Coatings*, 33(1), pp. 55-60. DOI: [http://doi.org/10.1016/S0300-9440\(98\)00008-3](http://doi.org/10.1016/S0300-9440(98)00008-3)
12. Belder, E.G., Rutten, H.J.J., Perera, D.Y. (2001) 'Cure characterisation of powder coatings', *Progress in Organic Coatings*, 42(3-4), pp. 142-149. DOI: [http://doi.org/10.1016/S0300-9440\(01\)00149-7](http://doi.org/10.1016/S0300-9440(01)00149-7)
13. Saad, G.R., Serag Eldin, A.F., (2012) 'Isothermal cure kinetics of uncatalysed and catalysed diglycidyl ether of bisphenol-A/carboxylated polyester hybrid powder coating' *Journal of Thermal Analysis and Calorimetry*, 110(3), pp. 1425-1430. DOI: <http://doi.org/10.1007/s10973-011-2074-8>
14. Ramis, X., Cadenato, A., Morancho, J.M., Salla, J.M. (2003) 'Curing of a thermosetting powder coating by means of DMTA, TMA and DSC', *Polymer*, 44(7), pp. 2067-2079. DOI: [http://doi.org/10.1016/S0032-3861\(03\)00059-4](http://doi.org/10.1016/S0032-3861(03)00059-4)
15. Wuzella, G., Kandelbauer, A., Mahendran, A.R., Müeller, U., Teisinger, A. (2014) 'Influence of thermos-analytical and rheological properties of an epoxy powder coating resin on the quality of coatings on medium density fibreboards (MDF) using in-mould technology', *Progress in Organic Coatings*, 77(10), pp. 1539-1546. DOI: <http://doi.org/10.1016/j.porgcoat.2013.10.016>
16. Thomas, A., Saleh, K., Guigon, P., Czechowski, C. (2009) 'Characterisation of electrostatic properties of powder coatings in relation with their industrial application', *Powder Technology*, 190(1-2), pp. 230-235. DOI: <http://doi.org/10.1016/j.powtec.2008.04.072>
17. Johnston, N.J., Cano, R.J., Marchello, J.M. Sandusky, D.A. (1995) 'Powder-coated towpreg: Avenues to near net shape fabrication of high performance composites', *Proceedings of ICCM10*, Whistler, BC, Canada, August. Vancouver: The Tenth International Conference on Composite Materials Society, pp 407 – 415.
18. Ramasamy, A., Wang, Y., Muzzy, J. (1996) 'Braided thermoplastic composites from powder-coated towpregs. Part I: Towpreg characterisation', *Polymer Composites*, 17(3), pp. 497-504. DOI: <http://doi.org/10.1002/pc.10639>

19. Nunes, J.P., Silva, J.F., Novo, P.J. (2013) 'Processing thermoplastic matrix towpregs by pultrusion', *Advances in Polymer Technology*, 32(S1), pp. E306-E312. DOI: <http://doi.org/10.1002/adv.21279>
20. Lionetto, F., Moscatello, A., Maffezzoli, A. (2017) 'Effect of binder powders added to carbon fiber reinforcements on the chemorheology of an epoxy resin for composites', *Composites Part B*, 112, pp. 243-250. DOI: <http://doi.org/10.1016/j.compositesb.2016.12.031>
21. Garschke, C., Parlevliet, P.P., Weimer, C., Fox, B.L. (2013) 'Cure kinetics and viscosity modelling of a high-performance epoxy resin film', *Polymer Testing*, 32(1), pp. 150-157. DOI: <http://doi.org/10.1016/j.polymertesting.2012.09.011>
22. Hardis, R., Jessop, J.L.P., Peters, F.E., Kessler, M.R. (2013) 'Cure kinetics characterization and monitoring of an epoxy resin using DSC, Raman spectroscopy, and DEA', *Composites: Part A*, 49, pp. 100-108. DOI: <http://doi.org/10.1016/j.compositesa.2013.01.021>
23. Kenny, J.M., Oplicki, M. (1993) 'Influence of the chemorheology of toughened epoxy matrices on the processing behaviour of high performance composites', *Makromolekulare Chemie. Macromolecular Symposia*, 63(1), pp. 41-56. DOI: <http://doi.org/10.1002/masy.19930680106>
24. Nijssen, R., de Winkel, G.D. (2016) 'Developments in materials for offshore wind turbine blades', in Ng, C. & Ran, L. (eds.) *Offshore Wind Farms. Technologies, Design and Operation*. Cambridge: Woodhead Publishing, pp. 85-104. DOI: <http://doi.org/10.1016/B978-0-08-100779-2.00005-2>
25. Flanagan, T., Maguire, J.M., Ó Brádaigh, C.M., Mayorga, P., and Doyle, A. (2015) 'Smart affordable composite blades for tidal energy', *Proceedings of EWTEC 2015 – 11th European Wave and Tidal Energy Conference*, Nantes, France, 6 – 11<sup>th</sup> September. European Wave and Tidal Energy Conference Series.
26. Stone, K.R., Springer Jr., G., (1995) *Advanced composites technology case study at NASA Langley Research Center*, Washington, DC, USA: U.S. Environmental Protection Agency.
27. Grunenfelder, L.K., Nutt, S.R. (2010) 'Void formation in composite prepregs – Effect of dissolved moisture', *Composites Science and Technology*, 70(16), pp. 2304-2309. DOI: <http://doi.org/10.1016/j.compscitech.2010.09.009>
28. Kim, D., Centea, T., Nutt, S.R., (2014) 'Out-time effects on cure kinetics and viscosity for an out-of-autoclave (OOA) prepreg: Modelling and monitoring', *Composites Science and Technology*, 100, pp. 63-69. DOI: <http://doi.org/10.1016/j.compscitech.2014.05.027>
29. Maguire, J.M., Doyle, A., Ó Brádaigh, C.M. (2017) 'Process modelling of thick-section tidal turbine blades using low-cost fibre reinforced polymers', *EWTEC 2017 - 12th European Wave and Tidal Energy Conference*, Cork, Ireland, 27<sup>th</sup> – 31<sup>st</sup> August. European Wave and Tidal Energy Conference Series.
30. Khoun, L., Centea, T., Hubert, P. (2009) 'Characterization methodology of thermoset resins for the processing of composite materials -- Case study: CYCOM 890RTM epoxy resin', *Journal of Composite Materials*, 44(11), pp. 1397-1415. DOI: <http://doi.org/10.1177/0021998309353960>
31. Schmidt, S., Mahrholz, T., Kühn, A., Wierach, P. (2016) 'Powder binders used for the manufacturing of wind turbine rotor blades. Part 1. Characterization of resin-binder interaction and preform properties', *Polymer Composites*, pp. 1-10. DOI: <http://doi.org/10.1002/pc.23988>
32. Daelemans, L., van der Heijden, S., De Baere, I., Muhammad, I., Van Paepegem, W., Rahier, H., De Clerck, K. (2015) 'Bisphenol A based polyester binder as an effective interlaminar toughener', *Composites Part B*, 80, pp. 145-153. DOI: <http://doi.org/10.1016/j.compositesb.2015.05.044>
33. ÉireComposites Teo. *GRN 918*. Product datasheet, 20 September 2013.
34. AkzoNobel. *Resicoat® HZH01R*. Product datasheet, 26 July 2016.
35. Chatterjee, A. (2009) 'Thermal degradation analysis of thermoset resins', *Journal of Applied Polymer Science*, 114(3), pp. 1417-1425. DOI: <http://doi.org/10.1002/app.30664>
36. Yousefi, A., Lafleur, P.G., Gauvin, R. (1997) 'Kinetic studies of thermoset cure reactions: A review', *Polymer Composites*, 18(2) pp. 157-168. DOI: <http://doi.org/10.1002/pc.10270>
37. Kamal, M.S. (1974) 'Thermoset characterisation for moldability analysis', *Polymer Engineering and Science*, 14(3), pp. 231-239. DOI: <http://doi.org/10.1002/pen.760140312>
38. Chern, C.S., Poehlein, G.W. (1987) 'A kinetic model for curing reactions of epoxides with amines', *Polymer Engineering & Science*, 27(11), pp. 788-795. DOI: <http://doi.org/10.1002/pen.760271104>



39. DiBenedetto, A.T. (1987) 'Prediction of the glass transition temperature of polymers: A model based on the principle of corresponding states', *Journal of Polymer Science Part B: Polymer Physics*, 25(9), pp. 1949-1969. DOI: <http://doi.org/10.1002/polb.1987.090250914>
40. Castro, J.M. (1980) *Mold filling and curing studies for the polyurethane RIM process*. PhD thesis. University of Minnesota.
41. Halley, P.J., Mackay, M.E. (1996) 'Chemorheology of Thermosets – An Overview', *Polymer Engineering and Science*, 36(5), pp. 593-609. DOI: <http://doi.org/10.1002/pen.10447>
42. Maguire, J.M., Roy, A.S., Doyle, D.A., Logan, M.G., Ó Brádaigh, C.M. (2015) 'Resin characterisation for numerical modelling of through-thickness resin flow during OOA processing of thick-section wind or tidal turbine blades', *Proceedings of ICCM20*, Copenhagen, Denmark, 19 – 24<sup>th</sup> July. International Committee on Composite Materials.
43. Kravchenko, O.G., Kravchenko, S.G., Pipes, R.B. (2016) 'Chemical and thermal shrinkage in thermosetting prepreg', *Composites: Part A*, 80, pp. 72-81. DOI: <http://doi.org/10.1016/j.compositesa.2015.10.001>
44. Centea, T., Hubert, P. (2012) 'Modelling the effect of material properties and process parameters on tow impregnation in out-of-autoclave prepregs', *Composites: Part A*, 43(9), pp. 1505-1513. DOI: <http://doi.org/10.1016/j.compositesa.2012.03.028>
45. Cender, T.A., Simacek, P., Advani, S.G. (2013) 'Resin film impregnation in fabric prepregs with dual scale permeability', *Composites: Part A*, 53, pp. 118-128. DOI: <http://doi.org/10.1016/j.compositesa.2013.05.013>
46. Kuentzer, N., Simacek, P., Advani, S.G., Walsh, S. (2006), 'Permeability characterisation of dual scale fibrous porous media', *Composites: Part A*, 37(11), pp. 2057-2068. DOI: <http://doi.org/10.1016/j.compositesa.2005.12.005>